

MODELLING AND OPTIMIZATION OF A CHILLED-WATER COOLING SYSTEM WITH MULTIPLE CHILLERS

by

Jiamin DU^a, Shuhong LI^{a*}, and Xinmei LI^b

^a School of Energy and Environment, Southeast University, Nanjing, China

^b Nanjing Fuca Automation Technology Co., Ltd., Nanjing, China

Original scientific paper

<https://doi.org/10.2298/TSCI200606328D>

In order to reduce energy consumption of the centralized chilled-water cooling system in large buildings, a dynamic control strategy was proposed for cooling plants by modelling and optimization. Combined with the chilled water flow model, this paper analyzed the parallel operation characteristics of the chillers and takes the load distribution as one of the control parameters. Based on the measured data of a typical cooling system that has undergone preliminary energy-saving transformation, the residual neural network is applied to model the relationship among energy consumption, controllable parameters and environmental parameters, and the residual neural network outperforms multi-layer perceptron and support vector regression. To minimize the total energy consumption, the gray wolf optimizer was introduced to optimize the controllable variables of the cooling system. Compared with the energy consumption before optimization, the simulation energy consumption after optimization decreased 10.45% on average, while the energy saving rate is only 7.9% with equal chilled water supply temperature of parallel chillers.

Key words: *chilled-water cooling system, modelling and optimization, cooling load distribution, energy conservation*

Introduction

The HVAC system is increasingly common in large-scale public buildings. While maintain comfortable indoor air environment, it accounts for 50~60% of the energy consumption required for building. The central chilled-water system, a subsystem of the HVAC system, consumes 60% of the total electricity of the HVAC system [1]. The central chilled-water system includes chillers, chilled water pumps, cooling water pumps, and cooling towers. Because of the changing weather condition, the uncertain quantity of the people, lead to the great fluctuation of the cooling load in the building. The settings of cooling plants are fail to dynamically controlled with the environmental parameters and cooling load demand, therefore, it has a large energy saving space [2].

The traditional control methods of HVAC system mainly include experience control, proportional integral derivate control, fuzzy control. The traditional methods have been widely applied in real system due to its cheap price. However, central chilled-water system is an extremely complex non-linear system, which has numerous plants and highly coupled operating parameters. The traditional control methods is difficult to achieve desired energy conservation effect [3]. In recent years, scholars have attempted to employ the heuristic optimization algorithm (such as genetic algorithm – GA, particle swarm optimization – PSO) to solve the

* Corresponding author, e-mail: equart@seu.edu.cn

operating parameters optimization problem. This method have to build the energy consumption estimation model first, there are many modelling methods which can be divided into three kinds: mechanism modelling, parameter identification modelling, and data-driven modelling. Wemhoff and Frank [4] applied lumped model to predict the energy savings of HVAC system, the validation results suggest that the lumped HVAC operate good. The model provide the basic for optimization of HVAC system, but a great number of theoretical formulas involved in the modelling process. The mechanism modelling method is too complex to be applied in actual project. Therefore, the mechanism model with undetermined coefficients was proposed. Vakiloroyaya *et al.* [5] developed a theoretical-empirical model to predict the performance of cooling plants over a wide range of operating conditions. The variables were determined by regression of field-test data collected. The experiment in real system suggest that the predicted data deviate from the actual data by higher than 10%. The parameter identification modelling method can satisfy the basic simulation demand, but the prediction accuracy is low. With the development of machine learning and the arrival of the big data era, data-mining technology are increasingly used in HAVC field. Neural network model has gradually become an important method for HVAC system modelling due to its efficiency and favorable accuracy compare to the conventional modelling approaches. Chen *et al.* [6] used the artificial neural network (ANN) to model the relationship among the power consumption of chiller, chilled water temperature, cooling water temperature and cooling load. According to the forecast result, the R^2 of the power consumption model by ANN was higher than that of the linear regression method (namely parameter identification modelling method), and the error percentage is lower. Based on the model, PSO was used to optimized the chiller loading, and obtain 12.68~17.63% energy saving as the load varies. Wang *et al.* [7] applied three different types of neural networks, namely radial basis function, multi-layer perceptron (MPL), support vector machine to model the component of the hybrid ejector air conditioning system. The MPL outperforms other two networks and produce the most accurate and steady component models in the research.

Due to heavy cooling load and control requirements, multi-chillers system is used as cooling system. The chillers most of time are under partial cooling load, and the law of energy efficiency varied with load is distinct for different plants. Therefore, minimize the energy consumption of chillers and determine the optimal load distribution is one of the research focus in HVAC system [8]. Chang *et al.* [9] established the relationship between COP and partial load rate of four chillers with different rated cooling capacity in a decoupled air conditioning system. The chilled water supply temperature as the variable and the evolution strategy was employed to solve optimal chiller loading problem. The simulated results presented evolution strategy method can save 0.98%-8.59% as the load varies. Yan *et al.* [10] mapped the relationship between the COP and the chiller capacity, chilled water return temperature, and cooling water return temperature by least-square method. Based on the model and GA, optimize the set-points of chilled water supply temperature according to the chilled water return temperature and chilled water flow collected in real time to optimize the cooling load distribution. The optimization results on the typical days of summer and transition season showed that the energy consumption of the chillers reduced by 25.75% and 5.35%, respectively, compared with the original operation mode.

In this paper, a cooling system with multi-chiller in a subway station was selected as the study object. Based on the collected real-time operating data, the residual neural network (ResNet) is applied to create a mapping among controllable parameters, environmental parameters and energy consumption. To minimize the power consumed by cooling plants, this paper establish the optimization model with operation principle, it take all independent controllable

variables into consideration, including cooling load distribution. Gray wolf optimizer (GWO) is employed to find the near optimal solution for control setting under different cooling demand. Optimized energy consumption and savings of each cooling plant is also discussed in the paper.

Data description

A real air conditioning chilled-water system of a subway station in a southern city in China is chosen as the case system. The total construction area of the station is 18776 m², the public area is 3342 m², and the total length of platform door is 113 m. The characteristics of each equipment is listed in tab.1. This system consists of two chillers, four cooling towers, four cooling water pumps, and four chilled water pump. The lay-out of the cooling plants is illustrated in fig. 1. The case system is a variable primary flow chilled water system, the chillers are connected in parallel and then in series with other plant groups. The system has environment management and control system (EMCS), which can accomplish real-time data collection, monitoring, security protection and operating control. The control strategy of EMCS includes: the set-points of the supply and return chilled water temperature were adjusted according to the pressure difference of the user side, the cooling water temperature set-point was automatically tuned according to the outdoor wet bulb temperature, and the cooling tower approximation. The statistical data suggested that the coefficient of performance of the central cooling system with EMCS was improved by 2.9% in June.

Table 1. Details of chillers

Equipment	ID	Characteristic
Chiller	WCC01	Nominal: cooling capacity = 813 kW, power = 116.9 kW, variable speed
	WCC02	Nominal: cooling capacity = 968 kW, power = 138 kW, variable speed
Cooling water pump	CWP01, CWP02	Nominal: flow rate = 176 m ³ /h, power = 15 kW, variable speed
	CWP03, CWP04	Nominal: flow rate = 106 m ³ /h, power = 7.5 kW, variable speed
Chilled water pump	CHWP01, CHWP02	Nominal: flow rate = 110 m ³ /h, power = 11 kW, variable speed
	CHWP03, CHWP04	Nominal: flow rate = 66 m ³ /h, power = 7.5 kW, variable speed
Cooling tower	CP01~CP04	Nominal: flow rate = 208 m ³ /h, power = 4.4 kW, variable speed

The data used in this research is collected from the EMCS during cooling period (6:30 a. m. to 23:30 p. m.) in summer. Because of the huge cooling load demand of the station under summer climate condition, two chillers, two chilled water pump (one large and one small), two cooling water pump (one large and one small) and four cooling tower are running. Figure 2 presented the cooling load changes over a day. The cooling demand was volatile, even it sometimes can meet by one chiller, two chillers remain running to avoid start and stop repeatedly. As a result, the chillers always in partial load. The real-time cooling load is calculated:

$$Q_e = \rho C M_{chw} (T_{chwb} - T_{chws}) \quad (1)$$

where ρ [kgm⁻³] is the density of chilled water, C [kJkg⁻¹°C⁻¹] – the specific heat of chilled water, M_{chw} [m³h⁻¹] – the flow rate of chilled water in the main pipe, T_{chws} [°C] – the chilled water supply temperature in the main pipe, and T_{chwb} [°C] – the chilled water return temperature in the main pipe.

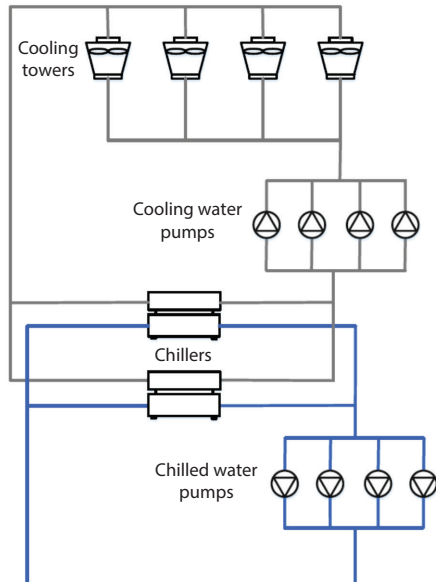


Figure 1. Lay-out of the central chilled water cooling system

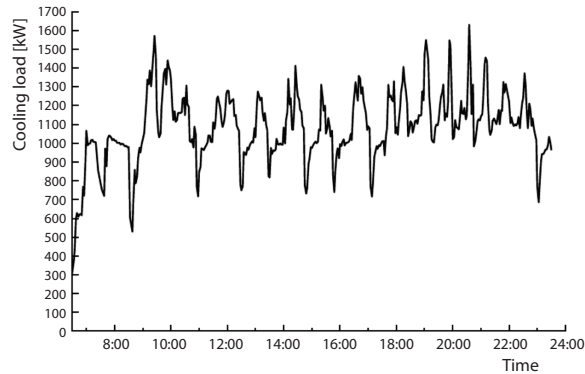


Figure 2. The real-time cooling load over a summer day

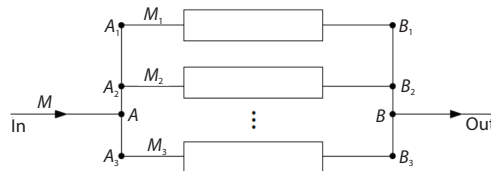


Figure 3. Schematic diagram of chilled water flowing through multiple chillers

Modelling

Chilled water flow distribution

In the case system, each pump are not directly connected to each chiller. As a result, only the total flow can be adjusted. It is necessary to obtain the quantity relationship between total flow and branch flow. Figure 3 shows the connection of the chilled water pipe-line when multiple chillers are running in parallel. Based on the Bernoulli equation of constant total flow, the chilled water energy equation at points A and B in fig. 3 is calculated:

$$z_{in} + \frac{P_{in}}{\gamma} + \frac{v_{in}^2}{2g} = z_{out} + \frac{P_{out}}{\gamma} + \frac{v_{out}^2}{2g} + h_{AB} \quad (2)$$

$$h_{AB} = SM^2$$

$$S = \frac{8}{\pi^2 d^4 g} \left(\frac{\lambda l}{d} + \sum \xi \right) \quad (3)$$

$$S_{AB} M^2 = S_{A_1 B_1} M_1^2 = S_{A_2 B_2} M_2^2 = \dots \quad (4)$$

$$M = M_1 + M_2 + \dots$$

where z_{in} and z_{out} are the heights of Points A and B in fig. 3, respectively, P_{in} and P_{out} – the pressure at the Points A and B, respectively, v_{in} and v_{out} – the velocities of chilled water through Points A and B, respectively, h_{AB} – the energy loss of chilled water flowing from A to B, can be seen as the product of resistance coefficient S_{AB} with the square of water flow rate M^2 . Due to the short pipe-line length of $A_1 A_2$, $A_2 A_3$, $B_1 B_2$, and $B_2 B_3$, the pressure difference between the two ends of each chiller can be considered to be equal, calculated by eq. (4) [9, 10]. Once the

total chilled water flow rate is determined, the water flow rate of each branch is determined accordingly. In conclusion, the resistance coefficient is the main factor affect the chilled water flow rate at the branch pipe.

Parallel operation characteristics of chillers

Figure 4 is the operating characteristic curve of WCC01 and WCC02 in case system (chilled water supply temperature is 9 °C, cooling water inlet temperature is 30 °C), where PLR represents the partial load ratio and COP is the coefficient of performance. It can be seen from fig. 4 that the COP increases with the increase of PLR, but the change ranges of the two chillers is different.

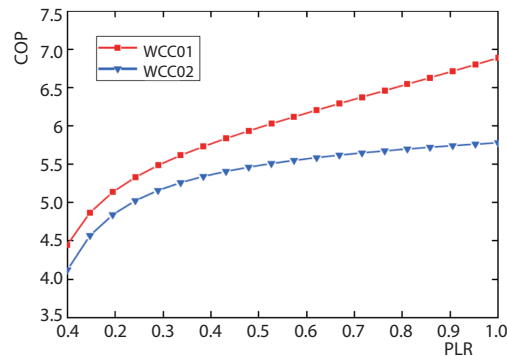


Figure 4. The COP vs. PLR

If the back water temperature of chilled water of each chiller is the same, the load distribution is related to the branch flow rate M_{chwj} and chilled water supply temperature T_{chwsj} , the cooling load of each chiller Q_j can determined by eq. (9). Since the branch flow distribution is only related to branch resistance coefficient, the cooling load distribution in this system is directly controlled by chilled water supply temperature difference between chillers:

$$PLR = \frac{\text{cooling} - \text{load}}{\text{cooling} - \text{capacity}} \tag{5}$$

$$COP = \frac{\text{cooling} - \text{load}}{\text{energy} - \text{consumption}} \tag{6}$$

$$Q_e = \sum_{j=1}^n Q_j \tag{7}$$

$$T_{chwb} = \frac{\sum_{j=1}^n M_{chwj} T_{chwsj}}{\sum_{j=1}^n M_{chwj}} + \frac{Q_e}{CM_{chw}} \tag{8}$$

$$Q_j = CM_{chwj} (T_{chwb} - T_{chwsj}) \tag{9}$$

Parameter selection

Adjustable parameters in a cooling system include number of plants, chilled water flow, cooling water flow, temperature of the cooling water enter into the chillers, each chiller's chilled water supply temperature, chilled water supply and return water temperature difference, and cooling water temperature difference between inlet and outlet water. This study focus on parallel operation condition so that the quantity of operational plants is certain. To select appropriate ones as control variables from above interrelated parameters, two commonly used

correlation analysis methods were applied to measure the relevance degree between operating parameters and energy consumption.

Pearson correlation coefficient [11] is a statistical method to investigate the correlation between two variables, the Pearson correlation coefficient between X and y can be calculated:

$$\rho(X, Y) = \frac{\text{cov}(X, Y)}{\sigma_X \sigma_Y} = \frac{\sum XY - \frac{\sum X \sum Y}{N}}{\sqrt{\left[\sum X^2 - \frac{(\sum X)^2}{N} \right] \left[\sum Y^2 - \frac{(\sum Y)^2}{N} \right]}} \quad (10)$$

where cov is the covariance, σX and σY are the standard deviation of X and Y , respectively, and N is number of corresponding variables.

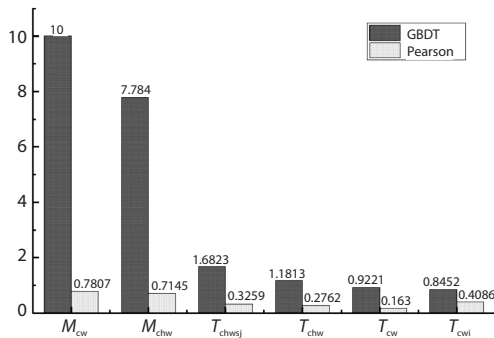


Figure 5. Influence value of different parameters on energy consumption

not directly involved, each different M_{chw} , T_{chwsj} corresponding to a different load distribution. The cooling load distribution is actually one of control variables. In addition, T_{air} , RH, and Q_e were used as the environmental variables of the simulation model.

Algorithm selection

The MLP and support vector regression (SVR) are most widely used neural network model in the simulation of HVAC system. The MLP originate from perceptron, it introduced one or more hidden layer based on a single layer perceptron neural network [13]. The training of MLP is to update weights by error back propagation. However, when the network reaches a certain depth, the network's characterization capability tends to be saturated, and the gradient disappears, which makes it impossible to train. The SVR is to map linear inseparable input data into a high dimensional linear separable feature space by kernel function and get the global optimal linear decision function [14]. It can avoid local optimization but the fitting effect depends on the choice of kernel function. Besides, when the training data size is great, it will be difficult to train.

He *et al.* [15] proposed a residual network based on ANN, introduced cross-layer connections between input and output, and divided the network into several residual units with the same architecture. If $F(X)$ is the original output of the network, the actual output with the shortcut structure would be $H(X) = F(X) + X$, that is, the input is added to the original output. The input information of each module can be transmitted across layers by stacking the residual modules, thus transforming the traditional identity maps into residual learning. It can alleviate

The gradient boosting decision tree (GBDT) [12] is one of the most representative ensemble learning algorithms which has high accuracy. It can output the relative importance of each feature after model training. The GBDT feature importance and the Pearson correlation coefficient of individual parameter are presented in fig. 5. The most important parameters are cooling water flow and chilled water flow, rest of parameters exhibited close importance. Considering that regulating temperature is more immediate than regulating temperature difference, select M_{chw} , M_{cw} , T_{cwi} , and T_{chwsj} as the control variables. Although cooling load distribution

the decline of network representational ability with deeper layers. Consequently, ResNet can be used for cooling plants modelling and may further enhance generalization capabilities and accuracy.

The common structure of the ResNet is shown in fig. 6. There are two fully connected layers in each residual unit, the input X passes through the first fully connected layer, and then output the $F^1(X)$ processed by batch normalization (BN) [16] and activation function, $Relu$, [17]. This output passes through the second fully connected layer and the batch normalization layer, then added to the input and passed to the activation function layer, finally output $F^2(X)$. The mathematical description:

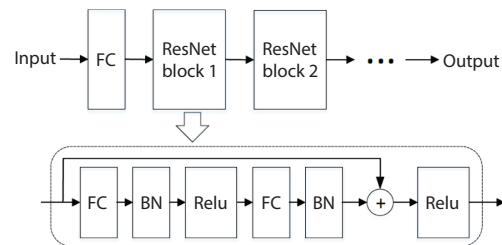


Figure 6. Structure of ResNet

$$F^1(X) = ReLU[BN(XW^1 + B^1)] \tag{11}$$

$$BN(x) = \frac{\gamma}{\sqrt{Var[x] + \epsilon}} \bullet x + \left(\beta - \frac{\gamma E[x]}{\sqrt{Var[x] + \epsilon}} \right) \tag{12}$$

$$ReLU(x) = \begin{cases} x, & x > 0 \\ 0, & x \leq 0 \end{cases} \tag{13}$$

$$F^2(X) = ReLU\{BN[F^1(X)W^2 + B^2] + X\} \tag{14}$$

where W^1, W^2, B^1 , and B^2 are the weight and bias of the two fully connected layers, respectively, $BN(\cdot), ReLU(\cdot)$ – the batch normalization function and activation function, respectively, $E[x], Var[x]$ – the mean and variance of x , respectively, and γ, β , and ϵ – the learnable reconstruction parameter of the normalization process.

Establishment and validation of cooling system model

The energy consumption of the cooling system is derived from its sub-components. Therefore, build the sub-model for components to integrated a whole system model will obtain more accurate optimization result. Besides, the ResNet model of chilled water flow was established to calculate the branch flow rate through each chiller. The input parameters, output parameters and network structure (determined by experiment) of each sub model are presented in tab. 2. In the table, M_{cw} – the chilled water flow, M_{chw} – the cooling water flow, T_{cwi} – the temperature of the cooling water enter into the chillers, and T_{chwsj} – the single chiller's chilled water supply temperature, ΔT_{chw} – the chilled water supply and return water temperature dif-

Table 2. Summary of component model

Model	Inputs	Outputs	Number of residual blocks	Number of neurons in each fully connected layer
Chilled water flow	M_{chw}	M_{chwj}	2	16
Chiller	Q_j, T_{chwsj}, T_{cwi}	$P_{chiller}$	4	64
Chilled water pump	M_{chw}	P_{chwp}	2	16
Cooling water pump	M_{cw}	P_{cwp}	2	16
Cooling tower	$T_{air}, RH, M_{cw}, T_{cwi}, Q_c$	P_{ci}	3	32

ference, ΔT_{cw} – the cooling water inlet and outlet water temperature difference, and Q_c – the condensation heat, approximately equals to the sum of the energy consumed by chillers and the refrigeration quantity. Figure 7 illustrate the coupling relationship of the sub models. The simulation programs were all written by python, the ResNet model was set up based on Keras (a deep learning framework).

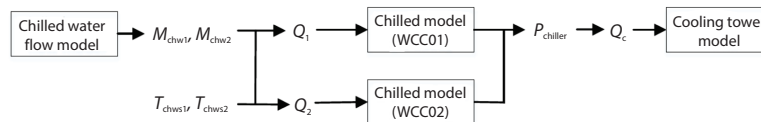


Figure 7. Schematic of the interrelationship between sub models

In this research, 25000 sets of sample data were selected to modelling and testing. Randomly scrambled the sample data and divided it into training samples and testing samples at a ratio of 7:3. In addition, the mean absolute percentage error (MAPE), mean absolute error (MAE), mean square error (MSE), and R^2 (goodness of fit) were introduced to evaluate the model:

$$MAPE = \frac{100\%}{n_s} \sum_{i=1}^{n_s} \left| \frac{\hat{y}_i - y_i}{y_i} \right| \quad (15)$$

$$MSE = \frac{1}{n_s} \sum_{i=1}^{n_s} (\hat{y}_i - y_i)^2 \quad (16)$$

$$MAE = \frac{1}{n_s} \sum_{i=1}^{n_s} |\hat{y}_i - y_i| \quad (17)$$

$$R^2 = 1 - \frac{\sum_{i=1}^{n_s} (y_i - \hat{y}_i)^2}{\sum_{i=1}^{n_s} (y_i - \bar{y})^2} \quad (18)$$

where y is the measured value \hat{y} – the predicted value, \bar{y} – the mean value of the measured data, and n_s – the number of samples.

As shown in fig. 8, the relative error of the chilled water flow model is less than 6%, which can meet the accuracy demand of cooling load distribution calculation. The prediction results of component models on 7500 test samples are shown in tab. 3, the MAE is in the range of 0.1~1.9, the MAPE is in the range of 1.4~9.6%, the MSE is in the range of 0.1~8.7, and the R^2 is higher than 0.83, indicating that the simulation models fit the inputs and outputs data very well. The prediction result of the total energy consumption is shown in fig. 9, the R^2 score is 0.9885, demonstrated that the ResNet model can simulate the non-linear relationship among control parameters, environmental parameters and energy consumption with excellent accuracy.

In order to compare the performance of the ResNet with traditional artificial neural network, this study chose two commonly used artificial neural network MLP, SVR to model with the same data. As the prediction results presented in tab. 4, the ResNet outperforms others in both testing and training sets.

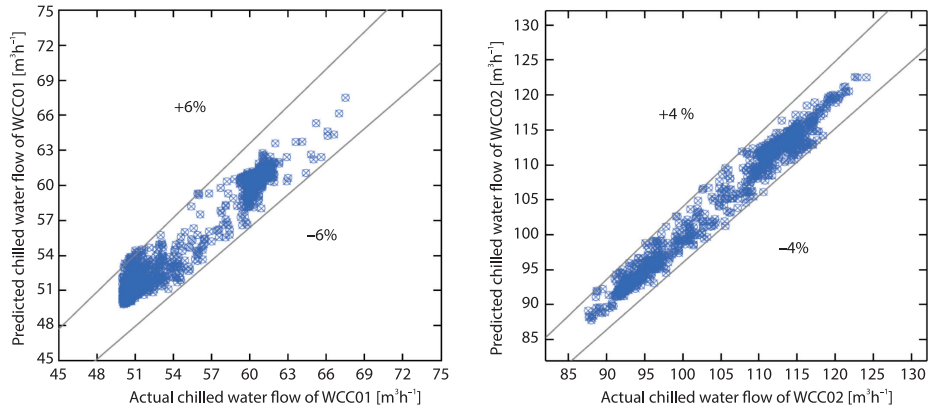


Figure 8. Prediction results of chilled water flow

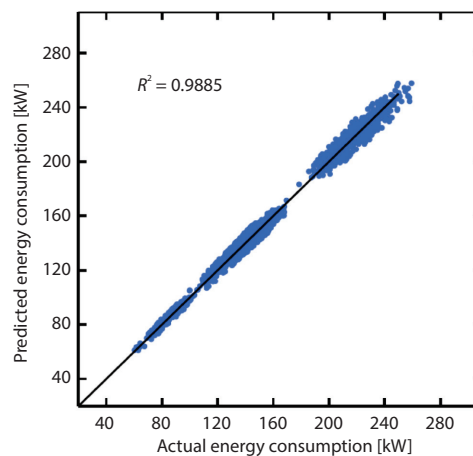
Table 3. Training and testing results of component models

Devices		MAE	MSE	MAPE	R^2
Chilled water pump	Testing	0.1008	0.0461	2.2034%	0.9764
	Training	0.0988	0.0448	2.1653%	
Cooling water pump	Testing	0.1762	0.1994	1.4748%	0.9963
	Training	0.1207	0.1549	1.1803%	
Cooling tower	Testing	0.2534	0.1259	9.5912%	0.8379
	Training	0.2083	0.0952	6.6978%	
WCC01	Testing	1.8081	8.7063	1.6495%	0.9832
	Training	1.5001	5.3881	1.3414%	
WCC02	Testing	0.2613	1.6990	1.6431%	0.9985
	Training	0.2147	1.3636	1.3266%	

Table 4. Training and testing results of ResNet, MLP, and SVR

Model		MAE	MSE	MAPE	R^2
ResNet	Testing	2.1381	12.0072	1.4613%	0.9885
	Training	2.0619	11.1463	1.3516%	
MLP	Testing	4.3956	31.0265	3.0444%	0.9703
	Training	4.3937	31.1673	3.0289%	
SVR	Testing	2.5016	13.0602	1.7568%	0.9875
	Training	2.3934	12.0330	1.6641%	

Figure 9. Prediction results of total energy consumption



Optimization model

Optimization model formulation

The energy consumption of the cooling system varied with the control parameters and environmental parameters. The established chilled-water cooling system model is used to construct the overall optimization model. The model optimize the set-points of control variables to minimize the energy consumption while meet the cooling load requirement. Thus the objective function is defined as the sum of the chiller energy, cooling water pump energy, chilled water pump energy and cooling tower energy, eq. (12):

$$M_{in}(P_{total}) \rightarrow \text{optimal}(M_{chw}, M_{cw}, T_{cwi}, T_{chwsj})$$

$$P_{total} = \sum_{j=1}^{n=2} P_{chiller}^{(j)} + \sum_{k=1}^2 P_{chw p}^{(k)} + \sum_{i=1}^2 P_{cwp}^{(i)} + \sum_{q=1}^4 P_{ct}^{(q)} \quad (19)$$

To ensure the calculated optimal results are in accordance with the actual operation, the constraints need to be satisfied are:

- In order to guarantee the chillers works, the chilled water supply temperature of each chiller should be within a certain range: $7 \leq T_{chws} \leq 12$ °C.
- To ensure the cooling tower works, the cooling water temperature enter into chillers should be within a certain range: $\max(27, T_{wb}) \leq T_{cwi} \leq 32$ °C.
- Cooling water loop and chilled water loop need to meet heat transfer constraints.

$$Q_c = Q_e + P_{chiller} = CM_{cw}(T_{cwb} - T_{cwi})$$

$$Q_e = CM_{chw}(T_{chw b} - T_{chws})$$

- In order to ensure the normal operation of the water system, the cooling and chilled water flow rate of the main and branch pipes would be within a certain range.

$$55 \leq M_{chw} \leq 180 \text{ m}^3/\text{h}$$

$$90 \leq M_{cw} \leq 300 \text{ m}^3/\text{h}$$

$$50 M_{cw1}, M_{cw1} \leq 190 \text{ m}^3/\text{h}$$

$$55 M_{chw1}, M_{chw2} \leq 130 \text{ m}^3/\text{h}$$

- In order to maintain indoor comfort, the chilled water supply temperature in the main pipe should meet the inequality [18]:

$$T_{chws} \leq \left(23.8 - 17 \frac{Q_e}{Q_{design}} \right) \text{°C}$$

Solution strategy of the optimization

The non-linear constrained optimization problem in this paper is too complex to solve by traditional mathematical programming method (such as Newton iterative method). The GA [19], PSO algorithm [20], differential evolution (DE) algorithm [21] and other swarm intelligence algorithms have been successfully used to solve optimization problems in air conditioning systems. The GWO algorithm is a new swarm intelligence algorithm inspired by the gray wolf's predation behavior and has few parameters, strong stability, and a mechanism for adjusting the convergence factor. Its accuracy and convergence speed have been proven to exceed

PSO in function optimization [22]. Therefore, the GWO is likely to obtain the nearer optimal solution and can be used for the dynamic optimization of the cooling system to maximize the energy-saving effect.

The GWO guides individuals to search optimal based on the positions of the first three wolves α , β , and δ . The position of each gray wolf corresponds to a solution. The detailed implementation steps are as follows.

Step 1. Input the environmental parameters of the optimized working conditions, set the variation range of the control parameters.

Step 2. Initialize parameters, set the population size p and the number of iterations r , and generate gray wolf population individuals randomly.

Step 3. Calculate the fitness value of gray wolf individuals. Divide the gray wolf population into α , β , δ , and ω according to their fitness.

Step 4. Update the position of the gray wolf individuals according to eq. (20), recalculate fitness value, and re-select the optimal wolves α , β , δ .

$$\begin{cases} \mathbf{D}_\alpha = |\mathbf{C}_1 \mathbf{X}_\alpha - \mathbf{X}| \\ \mathbf{D}_\beta = |\mathbf{C}_2 \mathbf{X}_\beta - \mathbf{X}| \\ \mathbf{D}_\delta = |\mathbf{C}_3 \mathbf{X}_\delta - \mathbf{X}| \end{cases}, \begin{cases} \mathbf{X}_1 = \mathbf{X}_\alpha - \mathbf{A}_1 (\mathbf{D}_\alpha) \\ \mathbf{X}_2 = \mathbf{X}_\beta - \mathbf{A}_2 (\mathbf{D}_\beta) \\ \mathbf{X}_3 = \mathbf{X}_\delta - \mathbf{A}_3 (\mathbf{D}_\delta) \end{cases} \quad (20)$$

$$\mathbf{X}(r_c + 1) = \frac{\mathbf{X}_1 + \mathbf{X}_2 + \mathbf{X}_3}{3}$$

where \mathbf{X} is the current position of the gray wolf individuals, r_s – the the current number of iterations, \mathbf{X}_α , \mathbf{X}_β , \mathbf{X}_δ – the current position of α , β , δ , \mathbf{D}_α , \mathbf{D}_β , \mathbf{D}_δ – the distance between the candidate wolf and α , β , δ , $\mathbf{A}_1 \sim \mathbf{A}_3$ and $\mathbf{C}_1 \sim \mathbf{C}_3$ – the synergy matrix, and $\mathbf{X}(r_s + 1)$ – the next position of the gray wolf individuals.

Step 5. If the iterations has reached the maximum, output the optimal gray wolf individual position, otherwise return to *Step 3*.

The fig. 10 is the flowchart of the optimization with GWO, the optimization program is written and implemented in Python. In the optimization process, it is necessary to discretize the continuous variables. The discrete step of M_{chw} , M_{cw} , T_{cwi} , T_{chwsj} are 5 m³/h, 5 m³/h, 0.1 °C, 0.1 °C. The outer point penalty function method is introduced to convert the constraint condition into a penalty term. So that the fitness value equals to the sum of the penalty term and the simulated total energy consumption of the system, eq. (21):

$$\text{fitness} = P_{\text{total}} + \text{punish} \quad (21)$$

Optimization results and discussion

To demonstrate the energy saving effect of the proposed method, 30 continuous points at a typical summer cooling day have been selected to show the optimization

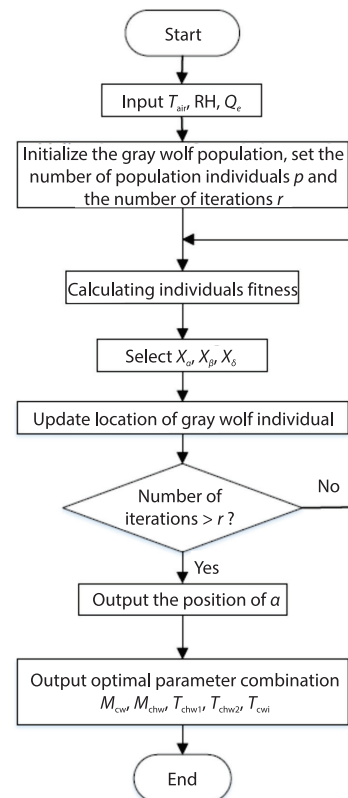


Figure 10. Flowchart of GWO algorithm

process. Figure 11 present the environmental parameters of the selected points, the cooling load changes within the range of 60-90% of the rated capacity. For each point, optimization model is established and solved by GWO. After several experiments, the number of iterations and populations are set as 200 and 50, respectively.

The six points with clear difference in cooling load were chosen to verify the performance of GWO. As shown in fig. 12, all optimization process reached convergence in 200 iterations. In addition, GA, PSO, and GWO were used to solve the optimization model of each point, and it was repeated 30 times. The statistical data of optimized system energy consumption by different optimization algorithm are listed in tab. 5. The lowest energy consumption in multiple calculations of three algorithms access to each other, but the deviation of GWO is smallest at every point. Together, the results indicated that GWO performs superb convergence on the cooling system optimization problem.

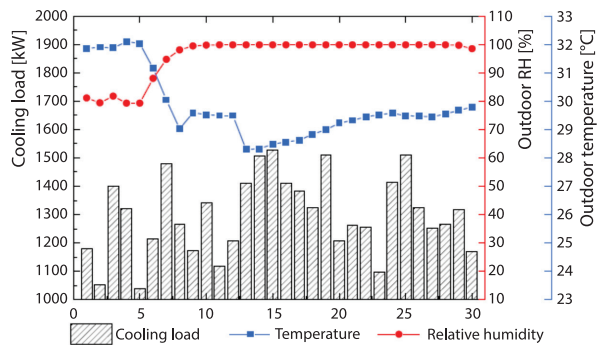


Figure 11. Environmental parameters of selected points

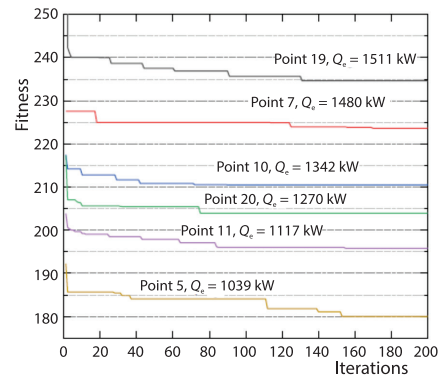


Figure 12. Fitness vs. iterations

The optimization results of operating parameters at 30 points are shown in fig. 13, and the corresponding optimized energy consumption of cooling plants and system are presented in figs. 14 and 15 (the simulated value represent the energy consumption predicted by ResNet model). The optimized energy consumption of cooling water pump significantly decreased with the decrease cooling water flow. The chilled water flow is associated with indoor comfort level, excessively low will cause the increase of chilled water back temperature. As a result, the chilled water flow and the energy consumption of chilled water pump have no significant decrease after optimization. The optimized energy consumption of cooling tower show a decreasing trend and it shares a low proportion of total power, it likely to sacrifice the energy-saving space of cooling tower for overall optimal energy efficiency. Chiller is the main energy-consuming equipment in chilled-water cooling system, reduce the energy consumption of chillers is crucial for the whole system. As shown in figs. 14 and 15, the change of the chiller energy consumption was same as that of the total energy. The optimized cooling water inlet temperature show a decreasing tendency, the chilled water supply temperature and the cooling load distribution has changed as presented in fig. 13, therefore, the average chiller energy consumption reduced by 8.14%.

Table 5. Energy consumption [kW] after optimization by GWO, GA, and PSO

Cooling load [kW]		GWO	GA	PSO
1511	Minimum	234.63	235.6	234.63
	Maximum	235.61	242.65	236.13
	Mean	234.84	236.87	234.70
1480	Minimum	223.65	223.65	223.65
	Maximum	223.75	224.98	234.43
	Mean	223.65	223.81	226.28
1342	Minimum	210.49	210.49	210.49
	Maximum	210.73	218.00	218
	Mean	210.50	210.84	211.06
1207	Minimum	203.94	203.94	203.94
	Maximum	204.11	209.50	209.8
	Mean	203.94	204.48	206.18
1117	Minimum	195.79	195.8	195.79
	Maximum	199.83	199.82	206.66
	Mean	196.06	198.34	197.04
1038	Minimum	180	180	180
	Maximum	180.34	183.53	188.54
	Mean	180.06	180.08	180.31

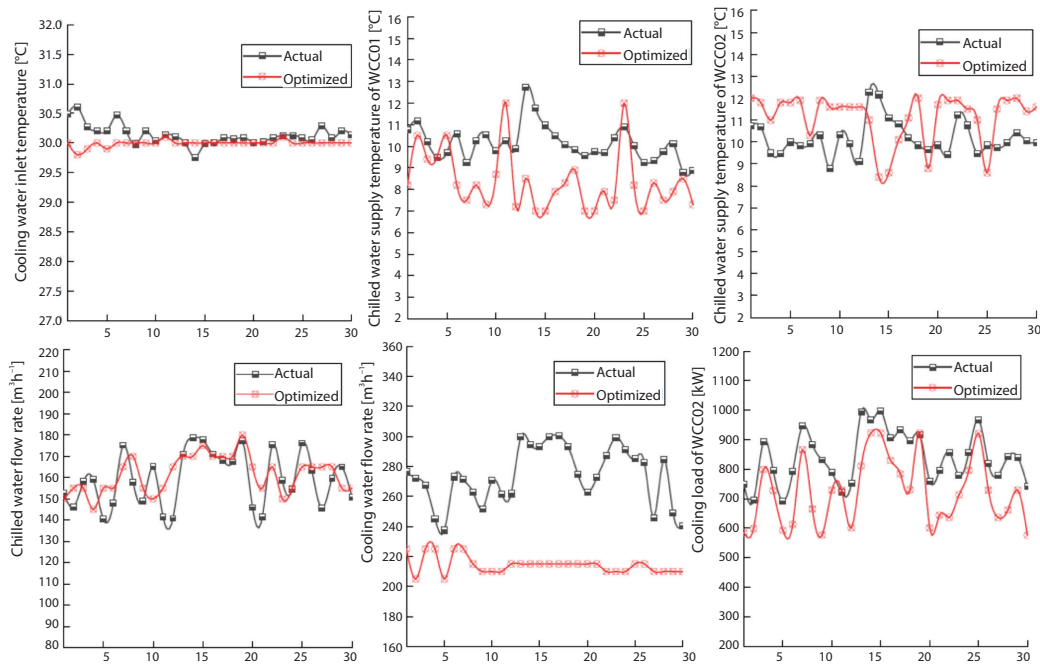


Figure 13. Operating parameters settings before and after optimization

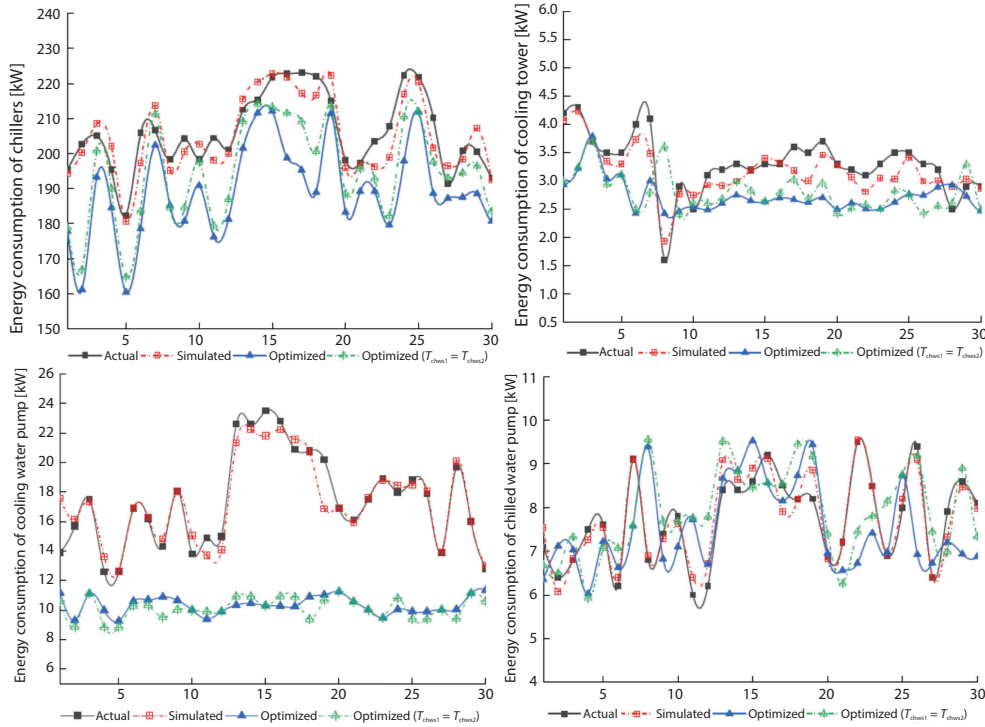


Figure 14. Cooling plants energy consumption before and after optimization

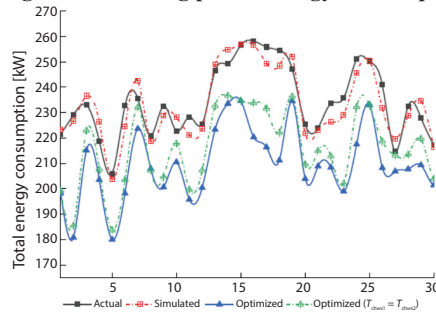


Figure 15. Total energy consumption before and after optimization

To analysis the impact of cooling load distribution on energy saving, the optimization model with equal chilled water supply temperature of all chillers ($T_{chws1} = T_{chws2}$) was formulated and solved by GWO at the same 30 points. As shown in figs.14, and 15, and tab. 6, the energy consumed by accessories (cooling towers, cooling water pumps and chilled water pumps) is very close to that of unequal chilled water temperature method. However, the energy-saving rate of chillers is significantly decreased. As a result, the total average energy-saving rate dropped from 10.45-7.9%.

Table 6. Average energy saving rate after optimization by two methods

Control variables	Cooling system	Chillers	Accessories
$M_{chws}, M_{cws}, T_{cwi}, T_{chws1}, T_{chws2}$	10.45%	8.14%	27.52%
$M_{chws}, M_{cws}, T_{cwi}, T_{chws}(T_{chws1} = T_{chws2})$	7.90%	5.37%	26.67%

Conclusion

This study established a optimization model of a chilled-water cooling system with multiple chillers by ResNet, the MAPE of the energy consumption simulation model in testing sets are 1.4613%, and its predict accuracy is higher than MLP, SVR, it has good generalization ability. To realize the energy-saving operation of the whole system, the GWO was introduced to solve the optimization model. The optimization results on typical parallel operation conditions showed a 10.45% energy savings of energy consumption even though the original operating condition has been optimized. However, the energy savings of chillers is severely reduced when the chilled water supply temperature of all chillers are equal, which indicated that the cooling load distribution is of great significance for the energy conservation of the parallel operation system.

References

- [1] Luis Perez-Lombard, et al., A Review on Buildings Energy Consumption Information, *Energy and Buildings*, 40 (2007), 3, pp. 394-398
- [2] Li, F. F., et al., Study of Public Building Energy Consumption Status and Energy Saving Potential, *Applied Mechanics and Materials*, 641-642 (2014), pp. 982-986
- [3] Yan, J. W., et al., Energy-Saving Optimization Operation of Central Air-Conditioning System Based on Double-DQN Algorithm, *Journal of South China University of Technology (Natural Science Edition)*, 47 (2019), 1, pp. 135-144
- [4] Wemhoff, A. P., Frank, M. V., Predictions of Energy Savings in HVAC Systems by Lumped Models, *Energy and Buildings*, 42 (2010), 10, pp. 1807-1814
- [5] Vakiloroyaya, V., et al., Modelling and Performance Prediction of an Integrated Central Cooling Plant for HVAC Energy Efficiency Improvement, *Building Simulation*, 6 (2013), 2, pp.127-138
- [6] Chen, C. L., et al., Applying Smart Models for Energy Saving in Optimal Chiller Loading, *Energy and Buildings*, 68 (2014)
- [7] Wang, H., et al., Modelling of a Hybrid Ejector Air Conditioning System Using Artificial Neural Networks, *Energy Conversion and Management*, 127 (2016), Nov., pp. 11-24
- [8] Zeng, Z., et al., Output Distribution of a Multiple Chiller System under Part Load Conditions, *HV and AC*, (2008), 3, pp. 107-110
- [9] Chang, Y. C., et al., Optimal Chiller Loading by Evolution Strategy for Saving Energy, *Energy and Buildings*, 39 (2007), 4, pp. 437-444
- [10] Yan, J., et al., Simulation Study on Optimal Load Distribution Strategy of Multiple Chillers, *HV and AC*, 46 (2016), 4, pp. 98-104-110
- [11] Benesty, J., et al., On the Importance of the Pearson Correlation Coefficient in Noise Reduction, *IEEE Transactions on Audio, Speech & Language Processing*, 16 (2008), 4, pp. 757-765
- [12] Friedman, J. H., Greedy Function Approximation: A Gradient Boosting Machine, *The Annals of Statistics*, 29 (2001), 5, pp. 1189-1232
- [13] Kalogirou, S. A., Applications of Artificial Neural-Networks for Energy Systems, *Applied Energy*, 67 (2000), 1-2, pp. 17-35
- [14] Chevalier, R. F., et al, Support Vector Regression with Reduced Training Sets for Air Temperature Prediction: A Comparison with Artificial Neural Networks, *Neural Computing & Applications*, 20 (2011), 1, pp. 151-159
- [15] He, K., et al., Deep Residual Learning for Image Recognition, *Proceedings*, 2016 IEEE Conference on Computer Vision and Pattern Recognition (CVPR), IEEE Computer Society, 2016
- [16] Ioffe, S., Szegedy, C., Batch Normalization: Accelerating Deep Network Training by Reducing Internal Covariate Shift, *Proceedings*, 32nd Int. Con. on Machine Learning, Lille, France, 2015, Vol. 37, pp. 448-456
- [17] Xu, B., et al., Empirical Evaluation of Rectified Activations in Convolutional Network, *Computer Science*, CoRR abs/1505.00853, 2015
- [18] Jinping, L., Zhou D., Energy Efficiency Analysis of Variable Chilled Water Temperature Adjustment in Air Conditioning Systems, *HV and AC*, (2004), 5, pp. 90-91 + 96
- [19] Lu, L., et al., THE HVAC System Optimization – in-Building Section, *Energy and Buildings*, 37 (2003), 1, pp. 11-22

- [20] Junqi, Y., *et al.*, Optimal Chiller Loading in HVAC System Using a Novel Algorithm Based on the Distributed Framework, *Journal of Building Engineering*, 28 (2020), Mar., 101044
- [21] Lee, W. S., *et al.*, Optimal Chiller Loading by Differential Evolution Algorithm for Reducing Energy Consumption, *Energy and Buildings*, 43 (2010), 2, pp. 599-604
- [22] Mirjalili, S., *et al.*, Grey Wolf Optimizer, *Advances in Engineering Software*, 69 (2014), Mar., pp. 46-61